Characterization of morphological alterations in micropapillary adenocarcinoma of the lung using an established cell line

DAI SONODA[1], KOKI KAMIZAKI[2], YUKIKO MATSUO[1], KANA ARUGA[2], MASASHI MIKUBO[1], KEISHI YAMASHITA[3], MICHIRU NISHITA[4], YASUHIRO MINAMI[2] and YUKITOSHI SATOH[1]

[1]Department of Thoracic Surgery, Kitasato University School of Medicine, Sagamihara, Kanagawa 252-0374; [2]Division of Cell Physiology, Department of Physiology and Cell Biology, Graduate School of Medicine, Kobe University, Kobe, Hyogo 650-0017; [3]Division of Advanced Surgical Oncology, Research and Development Center for New Medical Frontiers, Kitasato University School of Medicine, Sagamihara, Kanagawa 252-0374; [4]Department of Biochemistry, Fukushima Medical University School of Medicine, Fukushima, Fukushima 960-1295, Japan

Received August 5, 2021; Accepted October 20, 2021

DOI: 10.3892/or.2021.8230

Abstract. Micropapillary adenocarcinoma of the lung is a type of cancer associated with a poor prognosis and is characterized by the presence of tumor cells with a ring-like glandular structure floating within alveolar spaces. In the present study, the association between its morphological, biochemical and immunohistochemical characteristics, and malignancy was investigated using the KU-Lu-MPPt3 cell line established from a patient with MIP adenocarcinoma. Two subpopulations of KU-Lu-MPPt3 cells, namely adhesive (AD) and clumpy and suspended (CS) cells, were prepared and subjected to DNA microarray, reverse transcription-quantitative PCR, western blot and immunostaining analyses. Protein expression patterns were compared between the cell types and their derived tissues using immunostaining. The results revealed similar protein expression patterns between the tumor cells found in the alveolar spaces and CS cells, which exhibited morphological characteristic of MIP adenocarcinoma. Based on the results of DNA microarray analysis, the present study then focused on Akt and focal adhesion kinase (FAK), which were markedly activated in the KU-Lu-MPPt3 CS and AD cells, respectively. Following KU-Lu-MPPt3 CS cell plating onto collagen-coated culture dishes, some cells exhibited a transformation of their morphology into KU-Lu-MPPt3 AD-like cells within a few days, and their Akt and FAK activities were similar to those of the AD cells. Additionally, the inhibition of Akt and FAK activities with Akt and FAK inhibitors reduced KU-Lu-MPPt3 CS cell adhesion and proliferation. Thus, the aforementioned results indicated that the phosphorylation of FAK and Akt may play a crucial role in the regulation of KU-Lu-MPPt3 CS cell adhesion and proliferation, respectively. Furthermore, the malignant potential of MIP adenocarcinoma may be attributed to these morphological and biochemical alterations in the KU-Lu-MPPt3 cells.

Correspondence to: Professor Yukitoshi Satoh, Department of Thoracic Surgery, Kitasato University School of Medicine, 1-15-1 Kitasato, Minami-ku, Sagamihara, Kanagawa 252-0374, Japan
E-mail: ysatoh@med.kitasato-u.ac.jp

Abbreviations: AQP1, aquaporin 1; CD36, cluster of differentiation 36; FAK, focal adhesion kinase; Jak1, Janus kinase 1; MIP, micropapillary; PDK1, phosphoinositide-dependent protein kinase 1; TIMP1, tissue inhibitor of metalloproteinase-1; AD, adhesive; CS, clumpy and suspended; CAMs, cell adhesion molecules; CXCR4, C-X-C chemokine receptor type 4; ALDH1a, aldehyde dehydrogenase 1 family, member A1

Key words: Akt, cancer cell line, FAK, micropapillary lung adenocarcinoma, non-small cell lung cancer, tumor cluster

Introduction

Lung cancer has been the most commonly diagnosed type of cancer worldwide over the past several decades (1,2). The most common histological type of lung cancer is adenocarcinoma, consisting of the lepidic, acinar, papillary, micropapillary (MIP) and solid subtypes (3,4). Among these, MIP adenocarcinoma has been associated with frequent lymph node metastasis, lymphatic invasion, vascular invasion and a poor prognosis (5,6). This subtype was only recently proposed by the International Association for the Study of Lung Cancer, American Thoracic Society, and European Respiratory Society (IASLC/ATS/ERS) and formally added as a new subtype in the 2015 WHO classification (fourth edition) (4,7).

The MIP adenocarcinoma subtype is characterized by tumor cells growing in papillary tufts and forming florets that lack fibrovascular cores, detaching from and connecting to the alveolar walls. Generally, these tumor cells with ring-like glandular structures float within the alveolar spaces. However, the mechanism of the alveolar space localization of the tumor cells with ring-like glandular structures and its association with a poor prognosis of patients with MIP adenocarcinoma

have not yet been clarified. Furthermore, information on the pathophysiology of MIP adenocarcinoma and the development of therapeutic methods are limited due to the lack of sufficient research materials, such as cell lines, compared with other types of lung cancer.

The authors recently established the KU-Lu-MPPt3 cell line, the first established cell line of MIP adenocarcinoma, to the best of our knowledge (8). In the present study, a possible association of the characteristics of MIP adenocarcinoma with its malignancy was investigated by examining the KU-Lu-MPPt3 cells.

Materials and methods

Ethics statement. The present study was carried out in accordance with the Declaration of Helsinki and was approved by the Ethics Committee of Kitasato University Medical Ethics Organization (approval no. KME B09-33). The patient agreed to participate in the study and provided written informed consent, as in a previous study by the authors (8).

Cells and cell culture. The KU-Lu-MPPt3 MIP adenocarcinoma cell line was previously established in the authors' laboratory at Kitasato University (8). The KU-Lu-MPPt3 cells were cultured in Roswell Park Memorial Institute (RPMI)-1640 (Nacalai Tesque, Inc.) medium supplemented with 10% fetal bovine serum (FBS) on type I collagen-coated dishes (AGC Techno Glass Co., Ltd.) at 37˚C with 5% CO_2. The cells initially exhibited adherent cell morphologies at their establishment. Some cells then formed tufty aggregates and floated away from the adherent cells. The aggregated floating cells were collected and separately cultured from the adherent cells in tissue culture dishes. The KU-Lu-MPPt3 adherent cells were classified as KU-Lu-MPPt3 adhesive (AD) cells, and the aggregated floating cells were classified as KU-Lu-MPPt3 clumpy and suspended (KU-Lu-MPPt3 CS) cells (Fig. 1A). The ratio of KU-Lu-MPPt3 AD to KU-Lu-MPPt3 CS cells was not clear. However, the number of KU-Lu-MPPt3 CS cells was less than that of the KU-Lu-MPPt3 AD cells when some cells formed tufty aggregates and floated away from the adherent cells and became KU-Lu-MPPt3 CS cells. Mycoplasma testing was conducted for these cell lines and confirmed to be negative for mycoplasma infection (data not shown).

Microarray analysis. Total RNA was isolated from the KU-Lu-MPPt3 AD and CS cells using the RNeasy Mini kit (Qiagen GmbH) according to the manufacturer's protocol. Quality checks analysis on the RNA samples was performed using the Human Clariom D array (cat. no. 902915; Thermo Fisher Scientific, Inc.) gene chip. All results were analyzed using the Transcriptome Analysis Console 4.0.2 software (Thermo Fisher Scientific, Inc.). Gene expression profiles between the KU-Lu-MPPt3 AD and CS cells were compared. The fold change in expression was defined as the ratio of expression in KU-Lu-MPPt3 AD cells to that in KU-Lu-MPPt3 CS cells. Genes with ratios ≥2 were considered to be significantly differentially expressed.

Bioinformatics analysis. The DAVID 6.8 database (https://david.ncifcrf.gov/tools.jsp) was used to perform Kyoto Encyclopedia of Genes and Genomes (KEGG) pathway enrichment analysis. The species was limited to *Homo sapiens*.

Antibodies and inhibitors. The following reagents were purchased commercially: Anti-CD36 D8L9T (14347; Cell Signaling Technology, Inc.), anti-aquaporin 1 (AQP1) B-11 (cat. no. sc-25287; Santa Cruz Biotechnology, Inc.), anti-phosphorylated (p-)Akt (Ser473; cat. no. 9271; Cell Signaling Technology, Inc.), anti-Akt 40D4 (cat. no. 2920; Cell Signaling Technology, Inc.), anti-focal adhesion kinase (FAK) (H-1; cat. no. sc-1688; Santa Cruz Biotechnology, Inc.), anti-p-FAK (Tyr397; cat. no. 44-624G; Thermo Fisher Scientific, Inc.), anti-actin I-19 (cat. no. sc-1616; Santa Cruz Biotechnology, Inc.), Alexa Fluor-phalloidin (cat. no. A12379; Thermo Fisher Scientific, Inc.), Akt inhibitor X (cat. no. sc-203811; Santa Cruz Biotechnology, Inc.) and FAK inhibitor (PF-00562271; AdooQ BioScience).

Immunohistochemistry. The KU-Lu-MPPt3 AD cells treated with TrypLE Express Enzyme (Thermo Fisher Scientific, Inc.) and the CS cells were collected, embedded in iPGell (GenoStaff Co., Ltd.), and fixed with 10% formaldehyde neutral buffer solution at 4˚C overnight following the manufacturer's instructions. The lung cancer tissues were collected from the patient from whose tissue the KU-Lu-MPPt3 cells were established, and were paraffinized and cut into 4-μm-thick sections. All slides were subjected to autoclaving pretreatment for antigen retrieval using sodium citrate buffer (pH 6.0) and Tris-HCl buffer (pH 9.0). They were then blocked with Dako X0909 Protein Block, Serum-Free (Dako; Agilent Technologies, Inc.) at room temperature for 10 min, washed with PBS three times, and incubated with anti-CD36 (1:200 dilution), anti-AQP1 (1:100 dilution), anti-p-FAK (1:50 dilution) and anti-p-Akt (1:50 dilution) antibodies overnight at 4˚C. Subsequently, the cells were washed with PBS three times and incubated with secondary antibodies (MAX-PO MULTI, cat. no. 424151; Nichirei Biosciences Inc.) for 30 min at room temperature. The slides were then washed with PBS three times and stained with stable DAB (Thermo Fisher Scientific, Inc.) at room temperature (anti-CD36, 6 min; anti-AQP1, 10 min; anti-p-FAK, 5 min; anti-p-Akt, 6 min). The slides were washed once again and counterstained with hematoxylin (cat. no. 115938; Sigma-Aldrich, Inc.) for nuclear staining at 4˚C for 5 min. The slides were observed using an Olympus BX51 microscope (Olympus Corporation), and images were acquired using Olympus DP2-BSW software.

Immunofluorescence staining. The KU-Lu-MPPt3 CS cells were cultured on round coverslips coated with 1.8 mg/ml type I collagen (Koken Co., Ltd.) for 9 days, fixed in 10% formaldehyde neutral buffer solution for 10 min, washed with PBS three times, and permeabilized with 0.1% (v/v) Triton X-100 in PBS for 10 min at room temperature. After rinsing with PBS three times, the cells were blocked with 5% BSA at room temperature for 1 h. The cells were then incubated with anti-p-FAK (1:50 dilution) antibody overnight at 4˚C. The cells were then washed with PBS three times and incubated with secondary antibodies (cat. no. A11035; Thermo Fisher Scientific, Inc.) (1:200 dilution) and phalloidin (1:500 dilution) for 1 h at room temperature. After washing with PBS once again, the cells were labeled with 4,6-diamidino-2-phenylindole (DAPI)

(cat. no. D9542; Sigma-Aldrich, Inc.) for nuclear staining (1:1,000 dilution). A laser scanning confocal imaging system (LSM700; Carl Zeiss AG) was used to acquire fluorescence images. Three dimensional images were reconstituted using IMARIS software (Bitplane AG).

Western blot analysis. The cells were lysed in RIPA buffer (16488; Nacalai Tesque, Inc.) supplemented with a protease inhibitor cocktail (25955; Nacalai Tesque, Inc.) and phosphatase inhibitor cocktail solution II (FUJIFILM Wako Pure Chemical Corporation), to prepare whole-cell lysates. Protein concentrations were determined using a BCA protein assay kit (Thermo Fisher Scientific, Inc.). A total of 15 μg protein lysate was subjected to SDS-polyacrylamide gel electrophoresis (SDS-PAGE) using 10% SDS gel (cat. no. 414954; Cosmo Bio Co., Ltd.). The separated proteins were transferred onto a PVDF membrane and the membrane was blocked for 1 h at room temperature using blocking buffer (05999-84; Nacalai Tesque, Inc.), and incubated overnight at 4°C with primary antibodies against p-Akt (1:1,000 dilution), p-FAK (1:1,000 dilution), Akt (1:1,000 dilution), FAK (1:200 dilution) and actin (1:200 dilution). The membrane was then washed with PBST three times and incubated with secondary antibodies (anti-rabbit IgG: cat. no. 1706515; Bio-Rad Laboratories, Inc., anti-mouse IgG: cat. no. 1706516; Bio-Rad Laboratories, Inc., anti-goat: cat. no. A16005; Thermo Fisher Scientific, Inc.) (1:10,000 dilution) for 1 h at room temperature. Proteins were visualized and analyzed using an Image Quant LAS 4000 system with Image Quant TL7.0 analysis software imaging system (Cytiva). All western blot bands were semi-quantified using ImageJ 1.53i software (National Institutes of Health).

Cell proliferation assay. The KU-Lu-MPPt3 CS cells were cultured on collagen-coated 96-well plates (AGC Techno Glass Co., Ltd.) with or without inhibitors (Akt inhibitor X and FAK inhibitor PF-00562271) and incubated for 4 days at 37°C. The cells were then incubated with WST-8 (CCK-8; Dojindo Molecular Technologies, Inc.) at a final concentration of 10% (v/v), for 150 min at 37°C. The absorbances of the culture supernatants were measured at 450 nm using a SpectraMax M2 multifunctional microplate reader (Molecular Devices, LLC).

Cell adhesion assay. The KU-Lu-MPPt3 CS cells were plated onto collagen-coated 96-well plates with or without inhibitors (Akt inhibitor X and FAK inhibitor PF-00562271) and cultured for 3 days at 37°C in RPMI medium with 10% FBS. In preparation for the measurement of the numbers of attached cells, the wells were washed twice with PBS and filled with fresh medium containing 10% (v/v) WST-8. In preparation for the measurement of the total viable cell numbers, WST-8 was added without washing to the wells at a final concentration of 10% (v/v). Plates were then incubated for 150 min at 37°C, and the absorbances of the culture supernatants were measured at 450 nm using a SpectraMax M2 multifunctional microplate reader. The proportions of adherent cells were defined as the attached cell number/total cell number.

RNA isolation and reverse transcription-quantitative PCR (RT-qPCR). Total RNA was extracted from the KU-Lu-MPPt3 AD and CS cells using Sepasol-RNA I super G (Nacalai Tesque, Inc.) and subjected to reverse transcription to synthesize cDNA using the iScript™ cDNA Synthesis Kit (cat. no. 1708890; Bio-Rad Laboratories, Inc.). The reverse transcription conditions were as follows: 25°C for 5 min, 42°C for 30 min, 85°C for 5 sec, holding at 4°C. Thereafter, qPCR was performed using SYBR-Green (cat. no. 1725271; Bio-Rad Laboratories, Inc.) on a CFX96 Touch Real-time PCR Detection System (Bio-Rad Laboratories, Inc.) and *β-actin* was used as the internal reference gene. The PCR cycles were performed as follows: Initial denaturation at 95°C for 30 sec and then 40 cycles of 95°C for 10 sec and 60°C for 30 sec. A calibration curve (standard curve) was created and analyzed using the analysis was conducted with the $2^{-\Delta\Delta Cq}$ quantification method (9). The following primers were used: *CD36* forward, 5'-TGGGACCATTGGTGATGAG-3' and reverse, 5'-GCAACAAACATCACCACACC-3'; *AQP1* forward, 5'-TTTCTGTTTCCTGGCCTCAG-3' and reverse, 5'-TCCACAACTTCAAGGGAGTG-3'; 3-phosphoinositide-dependent protein kinase-1 gene *(PDK1)* forward, 5'-GAAGATGAGTGACCGAGGAGG-3' and reverse, 5'-GTAAAGACGTGATATGGGCAATC-3'; Janus kinase 1 gene *(Jak1)* forward, 5'-GGTCAGCATTAACAAGCAGGACAA-3' and reverse, 5'-AGCCATCTACCAGGGACACAAAG-3'; TIMP metallopeptidase inhibitor 1 *(TIMP1)* forward, 5'-TATCCATCCCCTGCAAACTG-3' and reverse, 5'-TTTTCAGAGCCTTGGAGGAG-3'; *Paxillin* forward, 5'-ACAGTCGCCAAAGGAGTC-3' and reverse, 5'-TGGTAGTGCACCTCACAGTA-3'; and *β-actin* forward, 5'-TCACCCACACTGTGCCCATCTACGA-3' and reverse, 5'-CAGCGGAACCGCTCATTGCCAATGG-3'.

Statistical analysis. All values are presented as the mean ± standard error, and all error bars represent the standard error of the mean. Statistical analysis was performed using JMP Pro 16 software (SAS Institute, Inc.). All results were analyzed using the unpaired Student's t-test and the one-way ANOVA followed by Dunnett's multiple comparison test. $P<0.05$ was considered to indicate a statistically significant difference.

Results

Comparison of MIP adenocarcinoma histopathological specimens and KU-Lu-MPPt3 cells. The KU-Lu-MPPt3 cell line was recently established by the authors as the first established MIP adenocarcinoma cell line, at least to the best of our knowledge (8). Although the cells adhere to and grow on collagen-coated dishes, some cells aggregate and float away from adherent cells during culture (Fig. 1A). To compare the characteristics of the KU-Lu-MPPt3 CS and AD cells, their gene expression profiles were examined, using DNA microarray analysis. In total, 8,054 genes were differentially expressed >2-fold, of which 3,882 and 4,172 genes were upregulated and downregulated, respectively (Table SI), in the KU-Lu-MPPt3 CS cells in comparison with the KU-Lu-MPPt3 AD cells. The most prominently differentially expressed genes are shown in Fig. 1B.

Among these genes, *CD36*, which encodes a fatty acid receptor (10), and *AQP1*, which has been reported to encode a water channel protein involved in the progression, invasion

A

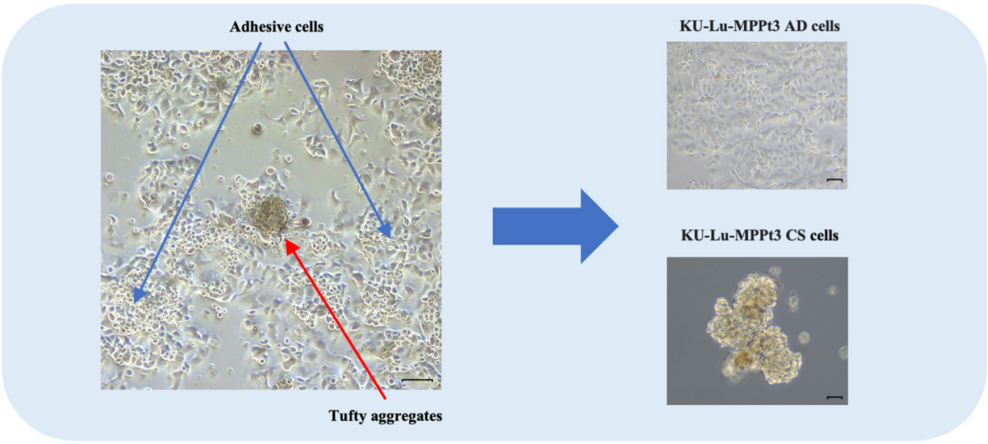

B

Description	KU-Lu-MPPt3 AD cells Avg (log2)	KU-Lu-MPPt3 CS cells Avg (log2)	Fold Change
CD36	6.88	17	-1116.15
AQP1	7.72	16.75	-523.46
PDK1	11.28	12.58	-2.47
Jak1	11.84	13.04	-2.3
Paxillin	13.7	11.91	3.46
TIMP1	12.36	5.2	142.5

C

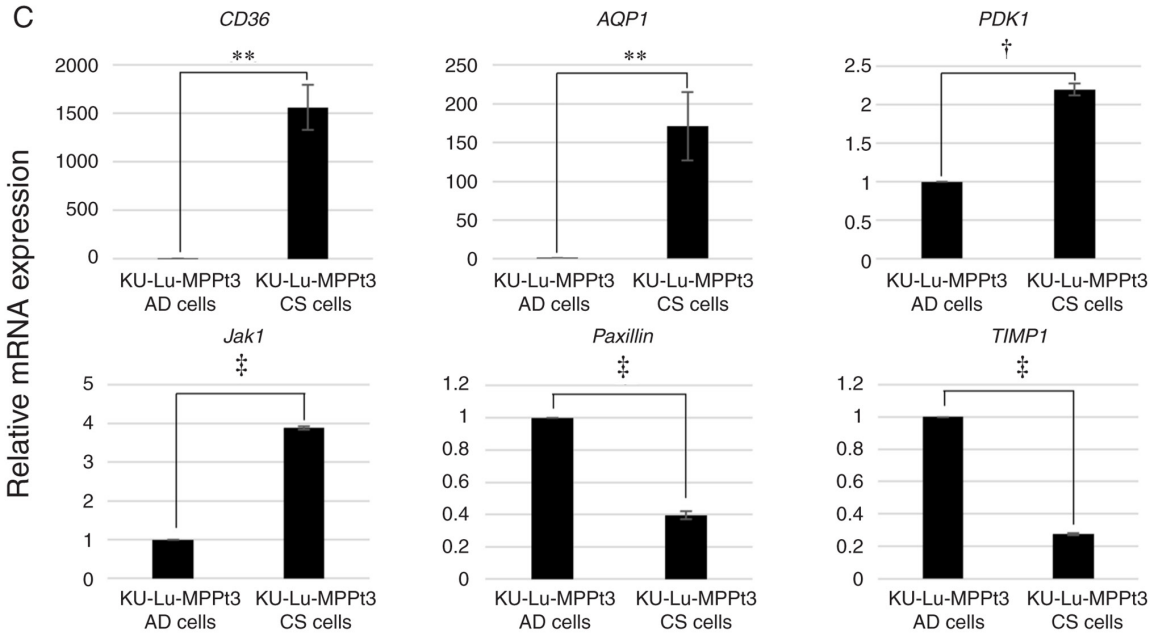

Figure 1. Preparation of KU-Lu-MPPt3 cell subpopulations and their differentially expressed genes. (A) Preparation of KU-Lu-MPPt3 cell subpopulations. Phase contrast images of original KU-Lu-MPPt3 cells (left panels) and their isolated subpopulations: AD cells and CS cells (right panels). Scale bar, 100 μm. (B) Differential expression levels of the indicated genes of the KU-Lu-MPPt3 AD and CS cells obtained using DNA microarray analysis. (C) Differential expression levels of the indicated genes of the KU-Lu-MPPt3 AD and CS cells obtained using reverse transcription-quantitative PCR. Data are expressed as the mean ± SE of three independent experiments. **P<0.01, †P<0.001 and ‡P<0.0001; determined using the t-test. AD, adhesive; CS, clumpy and suspended; AQP1, aquaporin 1; CD36, cluster of differentiation 36; Janus kinase 1; PDK1, phosphoinositide-dependent protein kinase 1; TIMP1, tissue inhibitor of metalloproteinase-1.

and metastasis of lung adenocarcinoma tumors (11), were highly expressed in the KU-Lu-MPPt3 CS cells (Fig. 1C). The *CD36* and *AQP1* differential expression levels at the protein level were then confirmed using immunohistochemistry. Their expression patterns were also compared with those of histopathological specimens from the patient with MIP adenocarcinoma. It was revealed that the KU-Lu-MPPt3 CS cells were positive for both CD36 and AQP1 proteins; however, the KU-Lu-MPPt3 AD cells were not (Fig. 2E, F, H and I). Several MIP component cells of the alveolar spaces in MIP adenocarcinoma specimens were positive for these proteins (Fig. 2D and G). Therefore, the KU-Lu-MPPt3 CS cells may retain properties similar to those of the characteristic tumor cells discovered in the alveolar spaces of patients with MIP adenocarcinoma. The tumor cells detected in the alveolar spaces have often been discovered in only a section

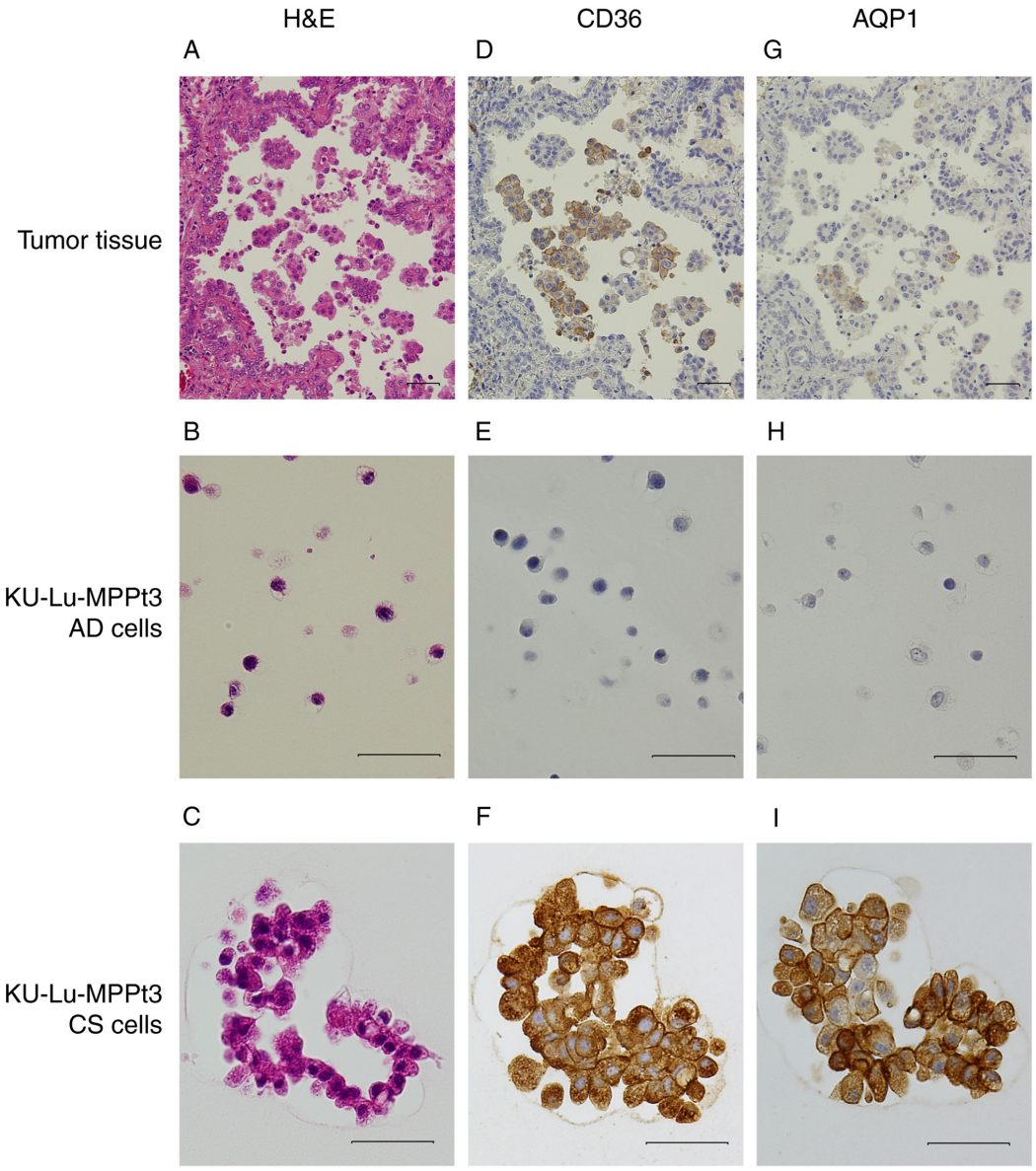

Figure 2. Expression of CD36 and AQP1 in KU-Lu-MPPt3 cell subpopulations and histopathological specimens. (A-C) Histopathological specimens of MIP adenocarcinoma and KU-Lu-MPPt3 AD and CS cells stained with H&E staining. (D-F) Histopathological specimens of MIP adenocarcinoma and KU-Lu-MPPt3 AD and CS cells stained with antibodies against CD36. (G-I) Histopathological specimens of MIP adenocarcinoma and KU-Lu-MPPt3 AD and CS cells stained with antibodies against AQP1. Scale bars, 50 μm. MIP, micropapillary; CD36, cluster of differentiation 36; AQP1, aquaporin 1; H&E, hematoxylin and eosin; AD, adhesive; CS, clumpy and suspended.

of MIP adenocarcinoma. Fewer KU-Lu-MPPt3 CS than KU-Lu-MPPt3 AD cells existing when certain cells are being separated from adherent cells and transforming into KU-Lu-MPPt3 CS cells is consistent with this clinical feature.

All differentially expressed genes identified in the microarray analysis were subjected to KEGG pathway enrichment analysis. Cell adhesion molecules (CAMs) and the Akt signaling pathway were among the enriched pathways. Among the genes identified using the microarray analysis, genes related to CAMs and the Akt signaling pathway were examined. CD36, PDK1 and Jak1, which were highly expressed in the KU-Lu-MPPt3 CS cells and have been associated with the activation of the Akt pathway (10,12-16), and paxillin and TIMP1, which were highly expressed in the KU-Lu-MPPt3 AD cells and are associated with the activation of the FAK pathway (17-20), were detected (Fig. 1B). Therefore, these genes were confirmed to be differentially expressed between the two cell types using RT-qPCR (Fig. 1C).

It was then examined whether Akt and FAK were differentially activated between the two cell types by performing western blot analysis with phospho-specific antibodies. It was demonstrated that the expression of total FAK was decreased in the KU-Lu-MPPt3 CS cells (Fig. 3A). Apart from this difference in total FAK levels, the p-FAK levels normalized to the total FAK levels were significantly decreased in the KU-Lu-MPPt3 CS cells (Fig. 3B). By contrast, whereas the total Akt levels were almost comparable between the KU-Lu-MPPt3 AD and CS cells (Fig. 3A), the normalized p-Akt levels were significantly increased in the KU-Lu-MPPt3 CS cells (Fig. 3B). Thus, the KU-Lu-MPPt3 CS cells exhibited a decreased and increased activity of FAK and Akt, respectively (Fig. 3A and B).

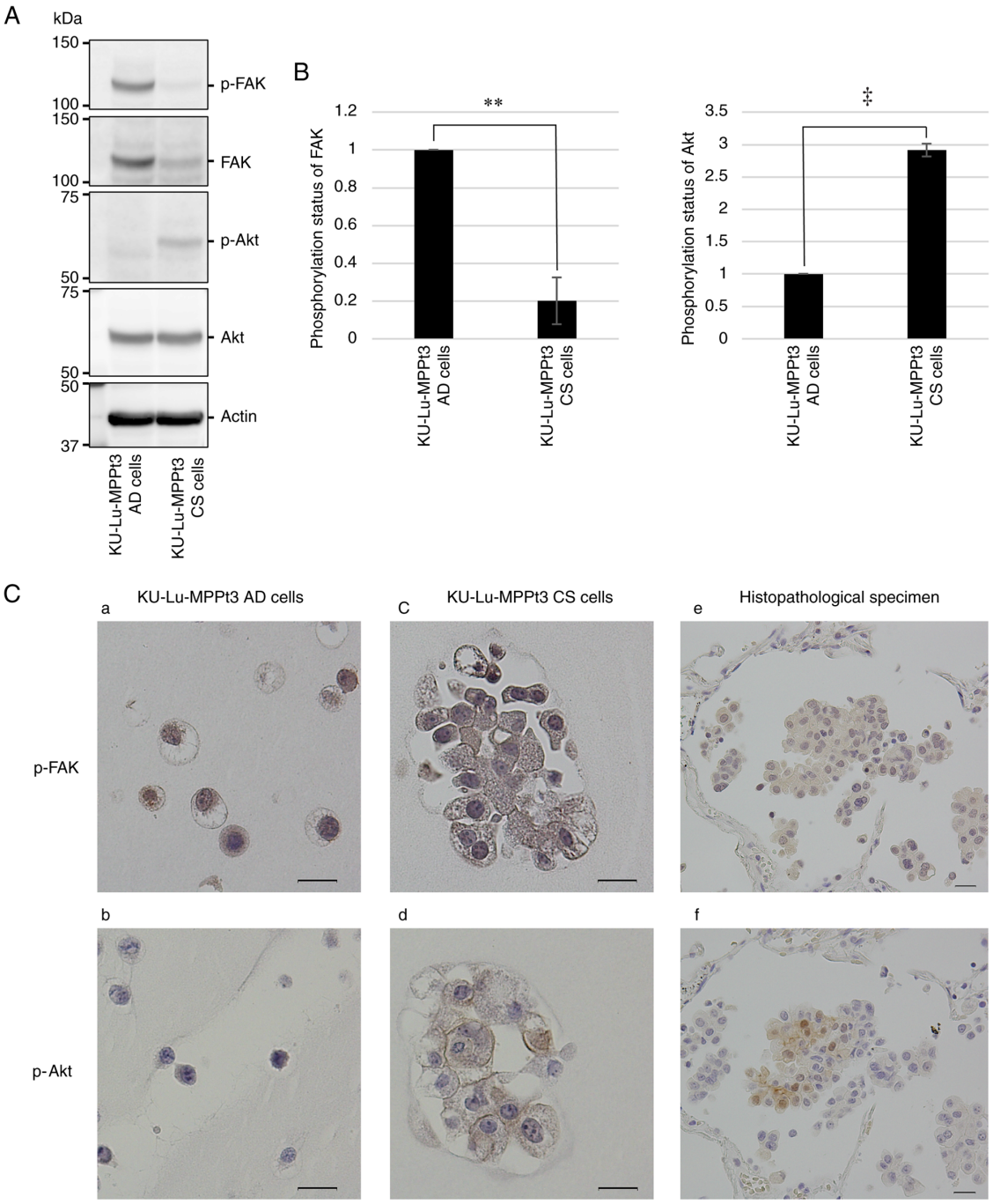

Figure 3. Differential phosphorylation of Akt and FAK amongst KU-Lu-MPPt3 cell subpopulations. (A) Evaluation of p-FAK (Tyr397) and p-Akt (Ser473) levels in KU-Lu-MPPt3 AD and CS cells using western blot analysis. (B) Relative quantification of p-FAK/total FAK and p-Akt/total Akt levels. Data are expressed as the mean ± SE of three independent experiments. (C) Immunohistochemical analysis of p-FAK and p-Akt in KU-Lu-MPPt3 AD cells (a and b), CS cells (c and d), and histopathological specimen (e and f). Scale bars, 20 μm. **P<0.01, ‡P<0.0001 determined using the t-test. AD, adhesive; CS, clumpy and suspended; FAK, focal adhesion kinase; p-FAK, phosphorylated FAK; p-Akt, phosphorylated Akt.

In the histopathological specimens, p-Akt was detected primarily in the MIP component cells in the alveolar space, being consistent with the results obtained for the KU-Lu-MPPt3 CS cells (Fig. 3C-d and -f). By contrast, p-FAK was detected in all tumor cells in the histopathological specimens, regardless of location (Fig. 3C-e). Since p-FAK was detected in both the KU-Lu-MPPt3 AD and CS cells at comparable levels (Fig. 3C-a and -c), the immunostaining performed herein may have failed to accurately quantify the levels of p-FAK. Furthermore, in addition to CD36, the expression of stem cell markers, such as SOX2, CD44, C-X-C chemokine receptor type 4 (CXCR4) and aldehyde dehydrogenase 1 family, member A1 (ALDH1a) was higher in the KU-Lu-MPPt3 CS cells than in the KU-Lu-MPPt3 AD cells in the microarray analysis, and similar results were obtained using RT-qPCR (unpublished data). The microarray data were uploaded in the National Center for Biotechnology Information Gene Expression Omnibus (GEO) database; GEO accession number GSE184883 (https://www.ncbi.nlm.nih.Gov/geo/query/acc.cgi?acc=GSE184883).

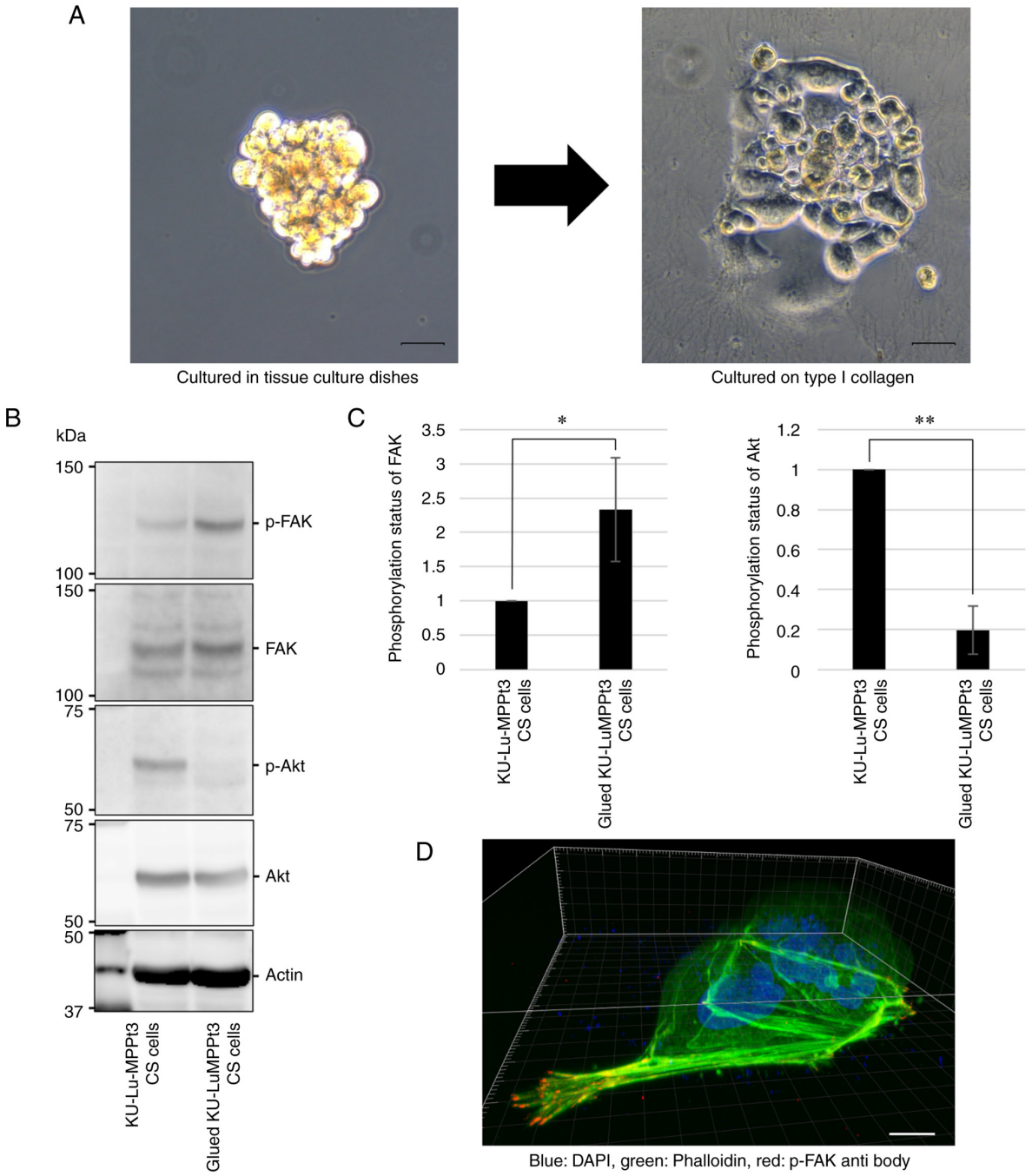

Figure 4. Changes in phosphorylation levels of Akt and FAK, following the attachment of KU-Lu-MPPt3 CS cells. (A) Phase-contrast images of KU-Lu-MPPt3 CS cells, cultured in tissue culture dishes (left panel) and culture dishes coated with type I collagen for 9 days (right panel). Scale bars, 100 μm. (B) Evaluation of p-Akt and p-FAK expression levels in glued KU-Lu-MPPt3 CS cells using western blot analysis. (C) Relative quantification of p-FAK/total FAK and p-Akt/total Akt levels. Data are expressed as the mean ± SE of three independent experiments. (D) Representative image of the glued KU-Lu-MPPt3 CS cells, cultured on round coverslips coated with type I collagen for 9 days and stained by anti-p-FAK antibody (red), phalloidin (green), and DAPI (blue). Scale bar, 20 μm. *P<0.05 and **P<0.01; determined using the t-test. FAK, focal adhesion kinase; p-FAK, phosphorylated FAK; p-Akt, phosphorylated Akt; CS, clumpy and suspended.

Morphological changes in the KU-Lu-MPPt3 CS cells following attachment to type I collagen. The KU-Lu-MPPt3 CS cells slowly proliferated in suspension when cultured in tissue culture dishes; however, when cultured on type I collagen, some cells changed their morphologies, resembling KU-Lu-MPPt3 AD cells within 9 days (Fig. 4A). Subsequently, several cells formed tufty aggregates with rising edges, of which specific cells detached and reverted to the KU-Lu-MPPt3 CS cell morphology (data not shown).

Thus, the Akt and FAK phosphorylation states between the KU-Lu-MPPt3 CS and transformed AD cells (hereafter referred to as glued KU-Lu-MPPt3 CS cells) were compared, following incubation on type I collagen-coated dishes at 37˚C for 9 days. Consistent with the cell morphology, the p-Akt and p-FAK levels were decreased and increased, respectively, in the glued KU-Lu-MPPt3 CS cells (Fig. 4B and C). Confocal microscopic analysis revealed that these cells formed lamellipodia-like protrusions with accumulated p-FAK

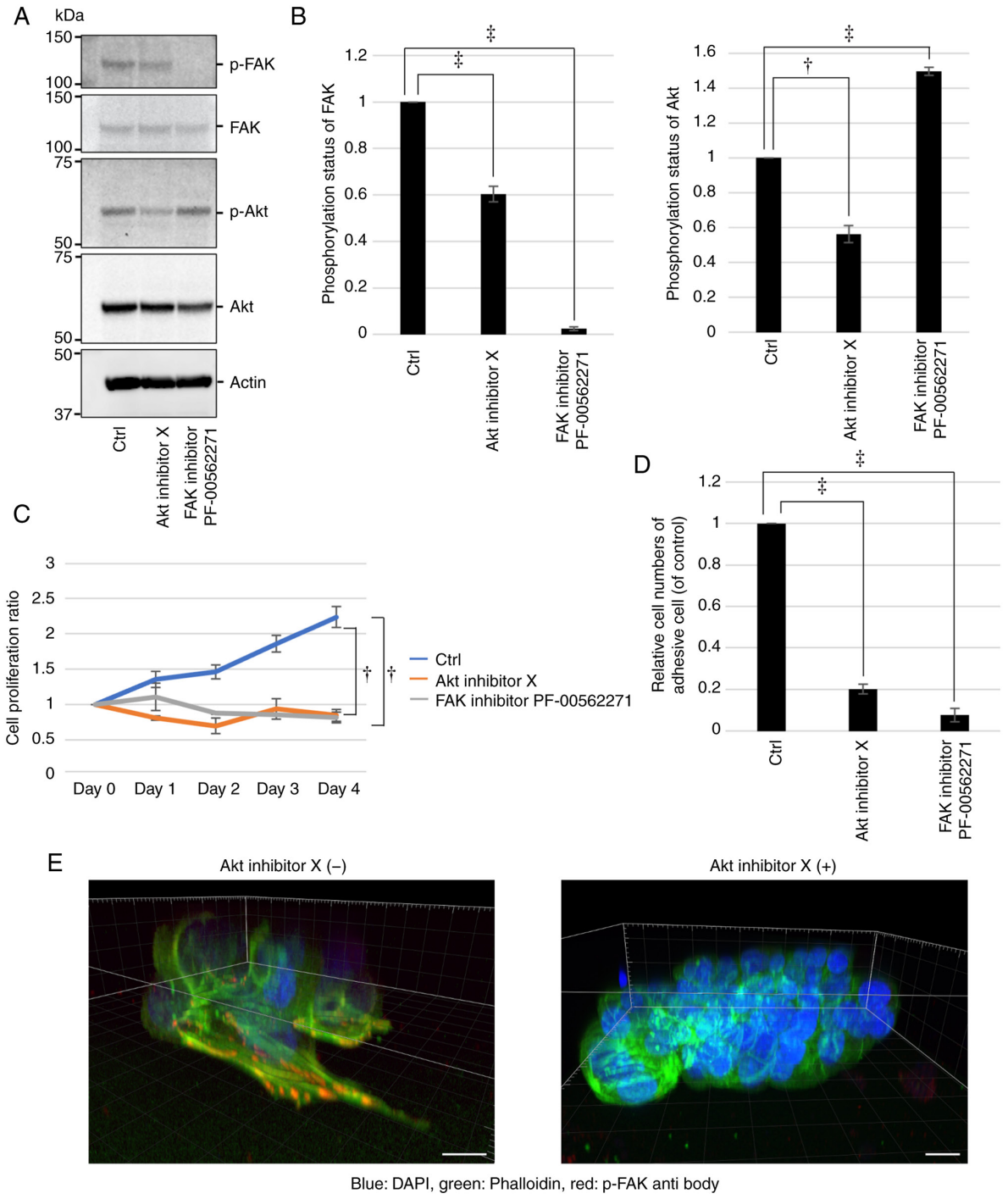

Figure 5. Akt activity is involved in the adhesion of KU-Lu-MPPt3 CS cells. (A) Evaluation of the effects of Akt inhibitor X and PF-00562271 FAK inhibitor on p-Akt and p-FAK expression levels using western blot analysis. (B) Quantification of p-FAK/total FAK and p-Akt/total Akt levels. Data are expressed as the mean ± SE of three independent experiments. (C) FAK or Akt inhibition effects on KU-Lu-MPPt3 CS cell proliferation. Data are expressed as the mean ± SE of three independent experiments. (D) FAK or Akt inhibition effects on KU-Lu-MPPt3 CS cell adhesion, as measured using WST-8 assay. Representative data are expressed as the mean ± SE of three independent experiments. (E) Three-dimensional confocal images of KU-Lu-MPPt3 CS cells cultured on round coverslips coated with type I collagen for 9 days in the presence (right panel) or absence (left panel) of Akt inhibitor X (20 μM). The cells were stained with anti-p-FAK antibody (red), phalloidin (green) and DAPI (blue). Scale bar, 20 μm. †P<0.001, ‡P<0.0001; determined using one-way ANOVA, followed by Dunnett's multiple comparison test. FAK, focal adhesion kinase; p-FAK, phosphorylated FAK; p-Akt, phosphorylated Akt; CS, clumpy and suspended.

(Fig. 4D). These findings suggest that the adhesiveness of the KU-Lu-MPPt3 cells was associated with their Akt and FAK activities.

Involvement of Akt and FAK in the adhesion and proliferation of KU-Lu-MPPt3 CS cells. It was further confirmed using western blot analysis that Akt and FAK inhibitors respectively decreased the p-Akt and p-FAK levels significantly in the KU-Lu-MPPt3 CS cells (Fig. 5A and B). Of note, it was also demonstrated that the Akt inhibitor decreased the p-FAK levels, whereas the FAK inhibitor increased the p-Akt levels (Fig. 5A and B), suggesting a possible signaling crosstalk

between Akt and FAK in the KU-Lu-MPPt3 cells. In order to investigate the involvement of Akt and FAK activities in the proliferation and adhesion of the KU-Lu-MPPt3 CS cells, the effects of Akt and FAK inhibitors on their proliferation and adhesion to type I collagen-coated plates were evaluated using the WST-8 assay. Although the untreated cells proliferated in type I collagen-coated plates, they failed to proliferate in the presence of either Akt or FAK inhibitors, presenting a significant decrease in cell numbers (Fig. 5C). Furthermore, both inhibitors markedly inhibited cell adhesion (Fig. 5D). The formation of lamellipodia-like protrusions with accumulated p-FAK was inhibited by the Akt inhibitor (Fig. 5E). These results suggested that the activities of both Akt and FAK are required for the adhesion and proliferation of KU-Lu-MPPt3 CS cells.

Discussion

MIP adenocarcinoma is a high-grade malignant tumor, presenting high rates of lymphatic invasion, visceral pleural invasion and lymph node metastases (5,6); it is also associated with a poor prognosis even in the early stages of the disease (6,21), and a high recurrence rate (22). Furthermore, patients with MIP-positive tumors tend to relapse locoregionally after limited resection (23,24). However, the biological mechanism underlying the progression of MIP adenocarcinoma has not yet been fully elucidated. Furthermore, there is no clear consensus on the mechanism and malignant effects of the characteristic ring-like glandular structure of tumor cells floating within alveolar spaces in MIP adenocarcinoma. By using immunohistochemistry, serial sectioning and electron microscopy, Kamiya *et al* (25) revealed that the micropapillary tufts appeared to float in alveolar spaces or spaces encased by connective tissues in histopathological sections. Furthermore, according to the serial sectioning in this previous study, most tufts were continuous with other tufts and the main tumor (25). In addition, it has also been reported that due to histopathological findings demonstrating no vascularity in micropapillary tufts, the route of nourishment for their constitutive cells was uncertain (25). On the other hand, another unique feature of MIP adenocarcinoma is the presence of non-integrated free tumor clusters, located away from the main tumors (26,27). However, this unique feature does not appear to be associated with the continuity of the identified tufts.

In the present study, it was observed that the cultured KU-Lu-MPPt3 CS cells shared morphological and immunohistological characteristics with the ring-like glandular structure of tumor cells floating within alveolar spaces. These cells appeared to survive in suspended states, ensuring nourishment from their surroundings. In addition, immunostaining of the pathological tissues revealed that the staining properties of the ring-like glandular structure of tumor cells floating within alveolar spaces were heterogeneous. Some cells demonstrated high levels of p-Akt, in similarity to the high levels of p-Akt in the KU-Lu-MPPt3 CS cells. These results suggested that two types of cells may exist in the ring-like glandular structure of tumor cells floating within alveolar spaces: One that maintains continuity with the alveolar wall and another one that can survive in a floating state without continuity with the alveolar wall, similar to the KU-Lu-MPPt3 CS cells. Non-integrated free tumor clusters may have been derived from floating tumors moving within the alveolar spaces, including KU-Lu-MPPt3 CS cells. It was demonstrated in the present study that the KU-Lu-MPPt3 CS cells not only survived in a suspended state, but also adhered and changed their morphology in the presence of appropriate substrates, in support of the clinical findings.

Of note, the KU-Lu-MPPt3 CS cells demonstrated a high p-Akt expression in suspended states, and Akt phosphorylation was observed to be a pre-requisite for adhesion. However, in the process of adhering and transforming into AD-like cells, the expression of p-FAK increased and expression of p-Akt decreased. Furthermore, by inhibiting the phosphorylation of Akt, the levels of p-FAK and the adhesive ability decreased. Furthermore, by inhibiting FAK phosphorylation, the p-Akt levels increased.

High levels of MIP adenocarcinoma malignancy may be attributed to the characteristic tumor cells within the alveolar spaces with the ring-like glandular structures. Furthermore, it may be attributable to its ability of directly infiltrating and changing morphology, in order to allow adhesion under appropriate conditions. Since Akt and FAK may be involved in this process, Akt or FAK activity inhibition may block the biological and pathological functions of MIP adenocarcinoma cells, including their growth.

In addition, several genes, including CD36, CD44, SOX2, CXCR4 and ALDH1a were upregulated in the KU-Lu-MPPt3 CS cells compared with the KU-Lu-MPPt3 AD cells, as determined using microarray analysis and RT-qPCR. These genes are known as cancer stem cell markers (28-34). Therefore, the KU-Lu-MPPt3 CS cells may have stem cell properties and this feature may also contribute to the malignancy of MIP adenocarcinoma. In future studies, the authors aim to evaluate the cancer stem cell like properties of the KU-Lu-MPPt3 CS cells.

Previous clinical trials have demonstrated that Akt inhibitors may be effective in the treatment of breast cancer (35,36). In addition, previously performed clinical trials on FAK inhibitors in patients with solid tumors have confirmed their safety and effectiveness, allowing the inhibitor application to proceed to clinical development (37,38). Thus, Akt and FAK inhibitors may be also useful therapeutic agents for the treatment of MIP adenocarcinoma. However, further assessment for these potential treatments is required.

A limitation of the present study is that in the microarray analysis, only one sample per cell was analyzed and the sample size was small. Therefore, the false discovery rate could not be determined. The number of samples will be increased and analysis will be performed in future studies.

In conclusion, the KU-Lu-MPPt3 CS cells, which share characteristics with MIP adenocarcinoma cells in the alveolar space, demonstrated high levels of p-Akt. Furthermore, it was revealed that their morphology may be altered under appropriate conditions, which was prevented by the administration of an FAK or Akt inhibitor. These morphological and biological features may be associated with the malignancy of MIP adenocarcinoma.

Acknowledgements

Not applicable.

Funding

The present study was supported in part by a grant from Parents' Association Grant of Kitasato University, School of Medicine, a grant-in-aid for Scientific Research (C) (20K07575) from MEXT, JST (Moonshot R&D) (JPMJMS2022), the Japan Agency for Medical Research and Development (AMED) (18gm5010001s0901), the Setsuro Fujii Memorial Osaka Foundation for Promotion of Fundamental Medical Research, and a grant-in-aid for Scientific Research (C) (19K09312) from MEXT.

Availability of data and materials

All microarray data were uploaded in the National Center for Biotechnology Information Gene Expression Omnibus (GEO) database; GEO accession number GSE184883 (https://www.ncbi.nlm.nih.Gov/geo/query/acc.cgi?acc=GSE184883). All remaining datasets used and/or analyzed during the current study are available from the corresponding author on reasonable request.

Authors' contributions

DS, KK, MN and YMi designed the experiments, analyzed the data and edited the manuscript. DS performed the majority of the experiments and assembled the data. KK, YMa and KA performed the immunofluorescence staining and microarray analysis. MM and KY analyzed the data and revised the manuscript. YS was involved in the conception and design of the experiments and supervised the whole experimental work and revised the manuscript. DS and KK confirm the authenticity of all the raw data. All authors have read and approved the final manuscript.

Ethics approval and consent to participate

The present investigation was approved by the ethics committee of Kitasato University Medical Ethics Organization (Approval No. KME B09-33). The patient agreed to participate in the study and provided written informed consent as per a previous study by the authors (8), and we did not use clinical specimen from anyone other than this patient in this study.

Patient consent for publication

Not applicable.

Competing interests

The authors declare that they have no competing interests.

References

1. American Cancer Society: Global Cancer Facts & Figures. 4th edition. American Cancer Society, Atlanta, GA, 2018.
2. Bray F, Ferlay J, Soerjomataram I, Siegel RL, Torre LA and Jemal A: Global cancer statistics 2018: GLOBOCAN estimates of incidence and mortality worldwide for 36 cancers in 185 countries. CA Cancer J Clin 68: 394-424, 2018.
3. Inamura K: Clinicopathological characteristics and mutations driving development of early lung adenocarcinoma: Tumor initiation and progression. Int J Mol Sci 19: 1259, 2018.
4. Travis WD, Brambilla E, Noguchi M, Nicholson AG, Geisinger KR, Yatabe Y, Beer DG, Powell CA, Riely GJ, Van Schil PE, *et al*: International association for the study of lung Cancer/American thoracic Society/European respiratory society international multidisciplinary classification of lung adenocarcinoma. J Thorac Oncol 6: 244-285, 2011.
5. Yoshida Y, Nitadori JI, Shinozaki-Ushiku A, Sato J, Miyaji T, Yamaguchi T, Fukayama M and Nakajima J: Micropapillary histological subtype in lung adenocarcinoma of 2 cm or less: Impact on recurrence and clinical predictors. Gen Thorac Cardiovasc Surg 65: 273-279, 2017.
6. Miyoshi T, Satoh Y, Okumura S, Nakagawa K, Shirakusa T, Tsuchiya E and Ishikawa Y: Early-stage lung adenocarcinomas with a micropapillary pattern, a distinct pathologic marker for a significantly poor prognosis. Am J Surg Pathol 27: 101-109, 2003.
7. World Health Organization: WHO Classification of Tumors of the Lung, Pleura, Thymus and Heart. Travis WD, Brambilla E, Burke AP, Marx A and Nicholson AG (eds). WHO/IARC Classification of Tumours. Lyon, IARC Publications, 2015.
8. Matsuo Y, Shiomi K, Sonoda D, Mikubo M, Naito M, Matsui Y, Yoshida T and Satoh Y: Molecular alterations in a new cell line (KU-Lu-MPPt3) established from a human lung adenocarcinoma with a micropapillary pattern. J Cancer Res Clin Oncol 144: 75-87, 2018.
9. Livak KJ and Schmittgen TD: Analysis of relative gene expression data using real-time quantitative PCR and the 2(-Delta Delta C(T)) method. Methods 25: 402-408, 2001.
10. Luo X, Zheng E, Wei L, Zeng H, Qin H, Zhang X, Liao M, Chen L, Zhao L, Ruan XZ, *et al*: The fatty acid receptor CD36 promotes HCC progression through activating Src/PI3K/AKT axis-dependent aerobic glycolysis. Cell Death Dis 12: 328, 2021.
11. Bellezza G, Vannucci J, Bianconi F, Metro G, Del Sordo R, Andolfi M, Ferri I, Siccu P, Ludovini V, Puma F, *et al*: Prognostic implication of aquaporin 1 overexpression in resected lung adenocarcinoma. Interact Cardiovasc Thorac Surg 25: 856-861, 2017.
12. Cifarelli V, Appak-Baskoy S, Peche VS, Kluzak A, Shew T, Narendran R, Pietka KM, Cella M, Walls CW, Czepielewski R, *et al*: Visceral obesity and insulin resistance associate with CD36 deletion in lymphatic endothelial cells. Nat Commun 12: 3350, 2021.
13. Gan G, Shi Z, Shangguan C, Zhang J, Yuan Y, Chen L, Liu W, Li B, Meng S, Xiong W and Mi J: The kynurenine derivative 3-HAA sensitizes hepatocellular carcinoma to sorafenib by upregulating phosphatases. Theranostics 11: 6006-6018, 2021.
14. Elsayed AM, Bayraktar E, Amero P, Salama SA, Abdelaziz AH, Ismail RS, Zhang X, Ivan C, Sood AK, Lopez-Berestein G, *et al*: PRKAR1B-AS2 long noncoding rna promotes tumorigenesis, survival, and chemoresistance via the PI3K/AKT/mTOR pathway. Int J Mol Sci 22: 1882, 2021.
15. Wang H, Hou W, Perera A, Bettler C, Beach JR, Ding X, Li J, Denning MF, Dhanarajan A, Cotler SJ, *et al*: Targeting EphA2 suppresses hepatocellular carcinoma initiation and progression by dual inhibition of JAK1/STAT3 and AKT signaling. Cell Rep 34: 108765, 2021.
16. Subotički T, Mitrović Ajtić O, Beleslin-Čokić BB, Bjelica S, Djikić D, Diklić M, Leković D, Gotić M, Santibanez JF, Noguchi CT and Čokić VP: IL-6 stimulation of DNA replication is JAK1/2 mediated in cross-talk with hyperactivated ERK1/2 signaling. Cell Biol Int 43: 192-206, 2019.
17. Deramaudt TB, Dujardin D, Noulet F, Martin S, Vauchelles R, Takeda K and Rondé P: Altering FAK-paxillin interactions reduces adhesion, migration and invasion processes. PLoS One 9: e92059, 2014.
18. Song M, Hu J and Quan HY: Abnormal expression of FAK and paxillin correlates with oral cancer invasion and metastasis. Acta Biochim Pol 68: 317-323, 2021.
19. Tang J, Kang Y, Huang L, Wu L and Peng Y: TIMP1 preserves the blood-brain barrier through interacting with CD63/integrin β 1 complex and regulating downstream FAK/RhoA signaling. Acta Pharm Sin B 10: 987-1003, 2020.
20. Song G, Xu S, Zhang H, Wang Y, Xiao C, Jiang T, Wu L, Zhang T, Sun X, Zhong L, *et al*: TIMP1 is a prognostic marker for the progression and metastasis of colon cancer through FAK-PI3K/AKT and MAPK pathway. J Exp Clin Cancer Res 35: 148, 2016.
21. Song Z, Zhu H, Guo Z, Wu W, Sun W and Zhang Y: Prognostic value of the IASLC/ATS/ERS classification in stage I lung adenocarcinoma patients-based on a hospital study in China. Eur J Surg Oncol 39: 1262-1268, 2013.

22. Yoshizawa A, Motoi N, Riely GJ, Sima CS, Gerald WL, Kris MG, Park BJ, Rusch VW and Travis WD: Impact of proposed IASLC/ATS/ERS classification of lung adenocarcinoma: Prognostic subgroups and implications for further revision of staging based on analysis of 514 stage I cases. Mod Pathol 24: 653-664, 2011.
23. Nitadori JI, Bograd AJ, Kadota K, Sima CS, Rizk NP, Morales EA, Rusch VW, Travis WD and Adusumilli PS: Impact of micropapillary histologic subtype in selecting limited resection vs lobectomy for lung adenocarcinoma of 2 cm or smaller. J Natl Cancer Inst 105: 1212-1220, 2013.
24. Tsubokawa N, Mimae T, Sasada S, Yoshiya T, Mimura T, Murakami S, Ito H, Miyata Y, Nakayama H and Okada M: Negative prognostic influence of micropapillary pattern in stage IA lung adenocarcinoma. Eur J Cardiothorac Surg 49: 293-299, 2016.
25. Kamiya K, Hayashi Y, Douguchi J, Hashiguchi A, Yamada T, Izumi Y, Watanabe M, Kawamura M, Horinouchi H, Shimada N, *et al*: Histopathological features and prognostic significance of the micropapillary pattern in lung adenocarcinoma. Mod Pathol 21: 992-1001, 2008.
26. Watanabe M, Yokose T, Tetsukan W, Imai K, Tsuboi M, Ito H, Ishikawa Y, Yamada K, Nakayama H and Fujino S: Micropapillary components in a lung adenocarcinoma predict stump recurrence 8 years after resection: A case report. Lung Cancer 80: 230-233, 2013.
27. Morimoto J, Nakajima T, Suzuki H, Nagato K, Iwata T, Yoshida S, Fukuyo M, Ota S, Nakatani Y and Yoshino I: Impact of free tumor clusters on prognosis after resection of pulmonary adenocarcinoma. J Thorac Cardiovasc Surg 152: 64-72.e1, 2016.
28. Erhart F, Blauensteiner B, Zirkovits G, Printz D, Soukup K, Klingenbrunner S, Fischhuber K, Reitermaier R, Halfmann A, Lötsch D, *et al*: Gliomasphere marker combinatorics: Multidimensional flow cytometry detects $CD44^+/CD133^+/ITGA6^+/CD36^+$ signature. J Cell Mol Med 23: 281-292, 2019.
29. Ghoneum A, Gonzalez D, Abdulfattah AY and Said N: Metabolic plasticity in ovarian cancer stem cells. Cancers (Basel) 12: 1267, 2020.
30. Yin Y, Xie CM, Li H, Tan M, Chen G, Schiff R, Xiong X and Sun Y: The FBXW2-MSX2-SOX2 axis regulates stem cell property and drug resistance of cancer cells. Proc Natl Acad Sci USA 116: 20528-20538, 2019.
31. Boumahdi S, Driessens G, Lapouge G, Rorive S, Nassar D, Le Mercier M, Delatte B, Caauwe A, Lenglez S, Nkusi E, *et al*: SOX2 controls tumour initiation and cancer stem-cell functions in squamous-cell carcinoma. Nature 511: 246-250, 2014.
32. Maréchal R, Demetter P, Nagy N, Berton A, Decaestecker C, Polus M, Closset J, Devière J, Salmon I and Van Laethem JL: High expression of CXCR4 may predict poor survival in resected pancreatic adenocarcinoma. Br J Cancer 100: 1444-1451, 2009.
33. Luo Y, Dallaglio K, Chen Y, Robinson WA, Robinson SE, McCarter MD, Wang J, Gonzalez R, Thompson DC, Norris DA, *et al*: ALDH1A isozymes are markers of human melanoma stem cells and potential therapeutic targets. Stem Cells 30: 2100-2113, 2012.
34. Chefetz I, Grimley E, Yang K, Hong L, Vinogradova EV, Suciu R, Kovalenko I, Karnak D, Morgan CA, Chtcherbinine M, *et al*: A Pan-ALDH1A inhibitor induces necroptosis in ovarian cancer stem-like cells. Cell Rep 26: 3061-3075.e6, 2019.
35. Kim SB, Dent R, Im SA, Espié M, Blau S, Tan AR, Isakoff SJ, Oliveira M, Saura C, Wongchenko MJ, *et al*: Ipatasertib plus paclitaxel versus placebo plus paclitaxel as first-line therapy for metastatic triple-negative breast cancer (LOTUS): A multicentre, randomised, double-blind, placebo-controlled, phase 2 trial. Lancet Oncol 18: 1360-1372, 2017.
36. Martorana F, Motta G, Pavone G, Motta L, Stella S, Vitale SR, Manzella L and Vigneri P: AKT inhibitors: New weapons in the fight against breast cancer? Front Pharmacol 12: 662232, 2012.
37. Soria JC, Gan HK, Blagden SP, Plummer R, Arkenau HT, Ranson M, Evans TR, Zalcman G, Bahleda R, Hollebecque A, *et al*: A phase I, pharmacokinetic and pharmacodynamic study of GSK2256098, a focal adhesion kinase inhibitor, in patients with advanced solid tumors. Ann Oncol 27: 2268-2274, 2016.
38. Mohanty A, Pharaon RR, Nam A, Salgia S, Kulkarni P and Massarelli E: FAK-targeted and combination therapies for the treatment of cancer: An overview of phase I and II clinical trials. Expert Opin Investig Drugs 29: 399-409, 2020.